Forensic Science International: Genetics 67 (2023) 102936

Contents lists available at ScienceDirect

Forensic Science International: Genetics

journal homepage: www.elsevier.com/locate/fsigen

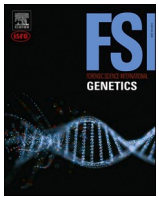

Development of an epigenetic age predictor for costal cartilage with a simultaneous somatic tissue differentiation system

A. Freire-Aradas [a,*], M. Tomsia [b], D. Piniewska-Róg [c], A. Ambroa-Conde [a], MA Casares de Cal [d], A. Pisarek [e], A. Gómez-Tato [d], J. Álvarez-Dios [f], E. Pośpiech [g,h], W. Parson [i,j], M. Kayser [k], C. Phillips [a], W. Branicki [e,l,**]

[a] Forensic Genetics Unit, Institute of Forensic Sciences, University of Santiago de Compostela, Spain
[b] Department of Forensic Medicine and Forensic Toxicology, Medical University of Silesia, Katowice, Poland
[c] Department of Forensic Medicine, Jagiellonian University Medical College, Kraków, Poland
[d] CITMAga (Center for Mathematical Research and Technology of Galicia), University of Santiago de Compostela, Spain
[e] Institute of Zoology and Biomedical Research, Jagiellonian University, Kraków, Poland
[f] Faculty of Mathematics, University of Santiago de Compostela, Spain
[g] Malopolska Centre of Biotechnology, Jagiellonian University, Kraków, Poland
[h] Department of Forensic Genetics, Pomeranian Medical University in Szczecin, Poland
[i] Institute of Legal Medicine, Medical University of Innsbruck, Austria
[j] Forensic Science Program, Pennsylvania State University, PA, USA
[k] Department of Forensic Molecular Biology, Erasmus MC University Medical Center Rotterdam, Rotterdam, the Netherlands
[l] Institute of Forensic Research, Kraków, Poland

ARTICLE INFO

Keywords:
DNA methylation
age estimation
costal cartilage
tissue identification
bone
blood
buccal cells

ABSTRACT

Age prediction from DNA has been a topic of interest in recent years due to the promising results obtained when using epigenetic markers. Since DNA methylation gradually changes across the individual's lifetime, prediction models have been developed accordingly for age estimation. The tissue-dependence for this biomarker usually necessitates the development of tissue-specific age prediction models, in this way, multiple models for age inference have been constructed for the most commonly encountered forensic tissues (blood, oral mucosa, semen). The analysis of skeletal remains has also been attempted and prediction models for bone have now been reported. Recently, the VISAGE Enhanced Tool was developed for the simultaneous DNA methylation analysis of 8 age-correlated loci using targeted high-throughput sequencing. It has been shown that this method is compatible with epigenetic age estimation models for blood, buccal cells, and bone. Since when dealing with decomposed cadavers or postmortem samples, cartilage samples are also an important biological source, an age prediction model for cartilage has been generated in the present study based on methylation data collected using the VISAGE Enhanced Tool. In this way, we have developed a forensic cartilage age prediction model using a training set composed of 109 samples (19–74 age range) based on DNA methylation levels from three CpGs in *FHL2*, *TRIM59* and *KLF14*, using multivariate quantile regression which provides a mean absolute error (MAE) of ± 4.41 years. An independent testing set composed of 72 samples (19–75 age range) was also analyzed and provided an MAE of ± 4.26 years. In addition, we demonstrate that the 8 VISAGE markers, comprising *EDARADD*, *TRIM59*, *ELOVL2*, *MIR29B2CHG*, *PDE4C*, *ASPA*, *FHL2* and *KLF14*, can be used as tissue prediction markers which provide reliable blood, buccal cells, bone, and cartilage differentiation using a developed multinomial logistic regression model. A training set composed of 392 samples (n = 87 blood, n = 86 buccal cells, n = 110 bone and n = 109 cartilage) was used for building the model (correct classifications: 98.72%, sensitivity: 0.988, specificity: 0.996) and validation was performed using a testing set composed of 192 samples (n = 38 blood, n = 36 buccal cells, n = 46 bone and n = 72 cartilage) showing similar predictive success to the training set (correct classifications: 97.4%, sensitivity: 0.968, specificity: 0.991). By developing both a new cartilage age model and a tissue differentiation model, our study significantly expands the use of the VISAGE Enhanced Tool while

* Corresponding author.
** Corresponding author at: Institute of Zoology and Biomedical Research, Jagiellonian University, Kraków, Poland.
E-mail addresses: ana.freire@usc.es (A. Freire-Aradas), wojciech.branicki@uj.edu.pl (W. Branicki).

https://doi.org/10.1016/j.fsigen.2023.102936
Received 14 April 2023; Received in revised form 13 September 2023; Accepted 27 September 2023
Available online 29 September 2023

increasing the amount of DNA methylation-based information obtained from a single sample and a single forensic laboratory analysis. Both models have been placed in the open-access Snipper forensic classification website.

1. Introduction

The identification of cadavers and human remains recovered from mass disaster events [1,2], exhumation [3–5], or missing persons identification [6] are among the many tasks performed by forensic geneticists. New technologies using biometric data, including machine learning methods, increasingly provide support for conventional human identification methods [7], but still the FBI and Interpol annually disclose their databases of unidentified remains [8,9]. According to the FBI's National Crime Information Center report for 2022, this database listed 546,568 missing person records. The 2022 records included 581 (64%) unidentified human cadavers, 5 (1%) unidentified mass disaster victims, and 316 (35%) living persons who could not ascertain their identity [8].

Costal cartilage tissue has been successfully used in cases of individual identification of corpses at an advanced stage of decomposition or with almost complete skeletonization and can be an alternative to soft tissue that has degraded DNA [10–12]. In fact, costal cartilage is one of the last tissues available for sampling before complete skeletonization occurs in human remains [13]. It is worth noting that cartilage tissue is a practical alternative forensic material to bone and teeth due to a much faster and cheaper DNA extraction procedure [10,14,15]. The advantages of using costal cartilage in the process of human identification has been shown in some cases because it may bypass the problem of chimerism [16,17]. In addition, cartilage tissue is increasingly chosen for other forensic analyses including forensic toxicology [18–21].

The hyaline tissue of the costal cartilage is the thickest cartilage in the human body. It connects the ribs to the sternum [22] has an abundant extracellular matrix that protects its DNA from environmental factors, and, amongst other material, consists of proteoglycans, and collagen I and II. As age increases, the quantity of type I collagen gradually decreases compared to type II collagen [23]. Pfeiffer et al. [24] demonstrated that the D/L aspartic acid ratios in the insoluble collagen fraction correlate with age ($r = 0.97$) and noted the 95% confidence interval around an estimated individual age was approximately 14 years. Other studies have shown that the extent of costal cartilage calcification (the measurement of calcification foci) might correlate with age [25,26]. Since the layer of hyaline tissue on long bone articular surfaces is much thinner, and thus more susceptible to degradation [27], the correlation between DNA methylation age and chronological age was found to be weaker ($r = 0.79$) and a median absolute difference of four years was estimated [28]. Age estimation can help identify decaying human remains by limiting the search criteria for a missing person but the forensic utility of a predictive method depends primarily on its accuracy [29]. It was found that epigenetic changes are essential in the aging process, and consequently DNA methylation (mDNA) has proven to be a very accurate measure of an individual's age. However, tissue specificity of DNA methylation patterns complicates the development of a universal epigenetic age predictor in forensics. The epigenetic age prediction has been explored more extensively for body fluids including blood and saliva which are often examined in criminal cases [30–32]. Recently, the VISAGE Consortium introduced the VISAGE Enhanced Tool for age prediction from somatic tissues based on eight most relevant methylation markers, covering 44 individual CpG sites. An assay based on target massively parallel sequencing (MPS) technology using the MiSeq system (Illumina, San Diego, CA, USA) was developed for simultaneous analysis of these markers enabling the collection of methylation data to predict age using specific algorithms for blood, buccal cells, as well as bone [32]. Age prediction models for blood, buccal cells and bone based on tissue-specific model training and testing datasets have been established providing prediction accuracies with mean absolute error of ± 3.2 to ± 3.7 years for the tissue-specific models.

A method of age prediction based on costal cartilage can be potentially useful in cases of identification of cadavers at an advanced stage of decomposition, when soft tissues or biological fluids are too degraded [33]. An additional reason for developing a predictive model for rib cartilage was that the models developed in our previous studies for blood, oral mucosa, and bone did not correctly predict the age of cartilage. Therefore, the present study aimed to develop a cartilage age prediction model based on three CpG sites analyzed with the VISAGE Enhanced Tool for age prediction from somatic tissues [32] using multivariate quantile regression as the predictive framework. A total of 109 costal cartilage samples ranging from 19 to 74 years were used to train the model. K-fold cross-validation was used for validation purposes, as well as an independent testing set composed of 72 samples from 19 to 75 years. Additionally, the VISAGE Enhanced Tool was adapted for tissue identification purposes covering the cell types targeted for age inference. Thus, a tissue prediction model for differentiating blood, buccal cells, bone, and cartilage was created using multinomial logistic regression based on a training set composed of 392 samples. We used k-fold cross-validation for validation, as well as a testing set composed of 192 samples, both training and test sets contained the four tissues of interest.

2. Material and Methods

2.1. Samples, DNA extraction, and quantification

The study was approved by the Bioethics Committee of the Jagiellonian University in Kraków, Poland (KBET/122.6120.86.2017). A total of 181 costal cartilage samples were collected during medicolegal autopsies at the Department of Forensic Medicine, Jagiellonian University Medical College in Krakow, Poland. The study group consisted of 145 males and 36 females in the age range of 19–75 years (mean 44.3 ± 14.6) and with a time from death to autopsy ranging from 1 to 5 days. The costal cartilage portions (5 × 6 cm) were collected from the cadavers' rib arches and stored at − 80 °C until further processing. Before starting the genetic analysis, the sampled material was cleaned by removing its external surface and any contamination, using a sterile scalpel, and then fragmented into small cubes. The fragmented tissue was placed in 1.5 ml Eppendorf tubes and incubated in an extraction mixture (Sherlock AX kit, A&A Biotechnology, Poland) at 50 °C in a Thermo–Shaker TS-100 C (Biosan) at 500 rpm for 24 h. Total DNA was extracted using a silica-based method with the Sherlock AX kit, according to the manufacturer's protocol. In addition, a total of 125 blood samples comprising 62 males and 63 females in the age range of 19–75 years old, (mean 48.9 ± 17.5); 122 buccal swabs comprising 62 males and 60 females in the age range of 19–80 years (mean 49.25 ± 17.9) and 156 bone samples comprising 125 males and 31 females in the age range of 19–75 years (mean 45.9 ± 14.4), were collected in the VISAGE project as described in Woźniak et al. [32] and used in this study. The quality and quantity of DNA isolates were measured using a NanoDrop 8000 UV-Vis Spectrophotometer and Qubit dsDNA HS Assay Kit on a Qubit 4 Fluorometer (Thermo Fisher Scientific, Waltham, MA, USA), following manufacturer's guidelines.

2.2. Bisulfite conversion, multiplex PCR, and massively parallel sequencing

Bisulfite conversion (BC) was performed with 500 ng of DNA using the EZ DNA Methylation-Direct Kit (Zymo Research, Irvine, CA, USA)

and then eluted in 25 μL.

DNA methylation levels were quantified using the VISAGE Enhanced Tool age prediction system [32]. The VISAGE MPS assay is based on PCR enrichment of targeted regions from bisulfite-converted DNA [34] and analyses of 44 CpG sites in eight age informative markers, namely *KLF14*, *TRIM59*, *MIR29B2CHG, FHL2*, *ELOVL2*, *EDARADD, PDE4C* and *ASPA*. In brief, 5 μL of the bisulfite-converted DNA samples were amplified in one multiplex PCR assay and libraries prepared using the KAPA Hyper Prep Kit and KAPA Unique-Dual Indexed Adapters (Roche, Basel, Switzerland). All samples were sequenced on the MiSeq instrument using the MiSeq Reagent Kit v3 (600 cycles) (Verogen, San Diego, CA, USA) with 2 × 150 cycles. Control and test samples were sequenced together in one run if the used indexes allowed multiplexing to avoid batch effects. Pooled libraries were diluted to 12pM and sequenced with a 10% PhiX spike.

Raw data in FASTQ files were aligned against a custom reference genome using a bwa-meth method as described in detail in Woźniak et al. [32]. The number of reads at the target positions were extracted using bam-readcount with a minimum mapping quality and minimum base quality set to 30 (https://github.com/genome/bam-readcount); DNA methylation levels were calculated as the ratio of C reads to the sum of C and T reads and expressed as a percentage (C reads/(C reads + T reads) * 100).

2.3. Statistical analyses

All calculations were performed using R software v.4.2.2 applying R scripts developed in-house. Spearman correlation (r_s) was used to assess correlations between DNA methylation levels and chronological age. Multivariate quantile regression with quantiles 0.1 and 0.9 was used to build the age prediction model with the *quantreg* R package [35]. The corresponding predictive accuracy was measured with the following performance metrics: mean absolute error (MAE) and root-mean-square error (RMSE). Although when working with quantiles, the MAE can be represented by the median instead of the mean, the mean was used in the present study for comparative purposes with additional models. Predicted versus chronological age was plotted using the *ggplot2* R package [36]. The final online cartilage age prediction model developed in our study has been placed in the open access Snipper forensic classification website and is freely available at: http://mathgene.usc.es/cgi-bin/snps3/age_tools/processmethylation-cartilage.cgi. Multinomial logistic regression was used for the development of the tissue prediction model using the *nnet* R package [37]. The corresponding predictive accuracy was measured with the following performance metrics: percent of correct classifications (%CC), sensitivity and specificity. Principal components were plotted using the *factoextra* R package [38]. Validation of the prediction models was performed using k-fold cross-validation (k = 10). The k-fold cross-validation system randomly cleaves input data into k fragments of similar sample size. Random cleavage of the input data was made using the *cvTools* R package [39]. Every k time that the model was assessed, a k cluster was retained as the test set with the remaining clusters used as the training set, maintaining proportions of 10% and 90% of the input data for test and training sets respectively, per run. The final online tissue prediction model developed in our study has been placed in the open access Snipper forensic classification website and is freely available at: http://mathgene.usc.es/cgi-bin/snps3/tissue_tools/processmethylation-tissue.cgi.

3. Results

3.1. CpG selection for age estimation in cartilage samples

A total of 44 CpGs located in eight genes (*KLF14*, *TRIM59*, *MIR29B2CHG, FHL2*, *ELOVL2*, *EDARADD, PDE4C* and *ASPA*) were analyzed in 181 costal cartilage samples. Specific information for the CpGs analyzed is outlined in Supplementary Table S1 and dispersion diagrams are shown in Supplementary Fig. S1. The corresponding DNA methylation data can be found in Supplementary Table S2. Three genes were discarded for the subsequent age estimation analyses due to a lack of, or weak correlation with age: *MIR29B2CHG*, *EDARADD* and *ASPA* (mean r_s: 0.04, −0.113 and 0.166, respectively). Patterns of hypermethylation were shown for the remaining five genes. The gene that had the highest correlation with age was *FHL2* for the CpG C4 (r_s: 0.931), followed by *TRIM59* for C7 (r_s: 0.906), *KLF14* for C3 (r_s: 0.888), *PDE4C* for C6 (r_s: 0.802) and lastly *ELOVL2* for C9 (r_s: 0.794). These eight CpG sites were initially selected for building the cartilage age prediction model.

3.2. Development of an age prediction model for cartilage samples

From a total of 181 costal cartilage samples, a subset of 109 (19–74 years old) was used for training the cartilage age prediction model. Multivariate quantile regression was tested with one-step increases in the total number of CpG sites included. The CpG sites were retained in the successive models following a decreasing order of correlation with age, and the addition of CpG sites stopped when no additional improvement was apported to the model. Table 1 shows the corresponding cross-validation performance metrics for the training set for the four assessed models (M1, M2, M3 and M4) In this way, the CpG with the highest Spearman correlation was assessed in the first model M1 (*FHL2*_C4), providing an MAE of ± 4.61 years and RMSE of 5.81. For the addition of a second CpG, *TRIM59*_C7 was analyzed (M2). Results obtained from M2 (*FHL2*_C4 and *TRIM59*_C7), provided an MAE of ± 4.47 years and RMSE of 5.76. The third most age-correlated CpG of *KLF14*_C3 was included in M3 (*FHL2*_C4, *TRIM59*_C7 and *KLF14*_C3) showing an MAE of ± 4.41 years and RMSE of 5.52. The fourth most age-correlated CpG was *PDE4C*_C6 included in M4 (*FHL2*_C4, *TRIM59*_C7, *KLF14*_C3 and *PDE4C*_C6). This model provided an MAE of ± 4.41 years and RMSE of 5.53. Since M4 do not improve the previous model M3, one-step increases were stopped at this point.

From these analyses, the optimum age prediction model was identified to be M3 (*FHL2*_C4, *TRIM59*_C7 and *KLF14*_C3) since this model provided the most accurate predictions. Therefore, M3 was selected as the final age prediction model for cartilage samples. To validate the final model, an independent subset of 72 samples (19–75 years old) was analyzed and provided an MAE of ± 4.26 years and RMSE of 5.39. Figs. 1A and 1B show the predicted age versus the chronological age for the training and test sets assessed with the M3 model. Continuous grey and black lines represent perfect and fitted correlations, respectively, while discontinuous black lines represent the age-specific prediction intervals. We detected correlation of the predicted with the chronological age with an R^2 value of 0.863 and 0.864 for the training and test sets, respectively. However, a slight overestimation of age in young

Table 1
Predictive performance metrics for the training (cross-validation) and test sets in cartilage for four age prediction models tested using quantile regression. MAE: Mean Absolute Error, RMSE (Root-Mean-Square Error). Bold indicates the selected model.

	Model	CpG nº	CpG_ID	MAE	RMSE
Training age cartilage (n = 109)	M1	1	*FHL2*_C4	± 4.61	5.81
	M2	2	*FHL2*_C4 *TRIM59*_C7	± 4.47	5.76
	M3	**3**	***FHL2*_C4** ***TRIM59*_C7** ***KLF14*_C3**	**± 4.41**	**5.52**
	M4	4	*FHL2*_C4 *TRIM59*_C7 *KLF14*_C3 *PDE4C*_C6	± 4.41	5.53
Test age cartilage (n = 72)	**M3**	**3**	***FHL2*_C4** ***TRIM59*_C7** ***KLF14*_C3**	**± 4.26**	**5.39**

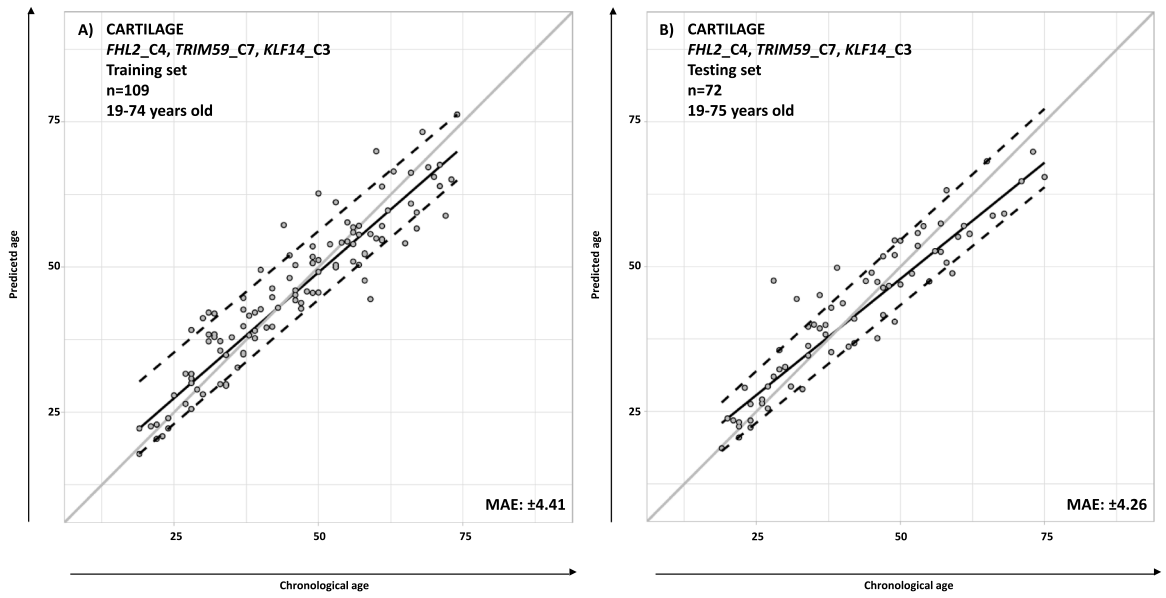

Fig. 1. Plot of predicted age against chronological age for cartilage in: **A)** the training set (n = 109, 19–74 years old); and **B)** the test set (n = 72, 19–75 years). Predicted age was inferred from a multivariate quantile regression model based on three CpG sites (*FHL2*_C4, *TRIM59*_C7 and *KLF14*_C3). The black diagonal line represents the 0.5 quantile regression line between predicted age and chronological age and the discontinuous black lines, the corresponding 0.1 and 0.9 quantile regression limits (prediction intervals). The grey line is the diagonal line representing perfect correlation.

individuals as well as a moderate underestimation in older samples is observed in the test set.

The following equation describes the multivariate quantile regression model M3:

Predicted age in years = −0.79 + (0.65 x *FHL2*_C4) + (0.04 x *TRIM59*_C7) + (2.05 x *KLF14*_C3).

Prediction intervals were estimated using the following equations:

Minimum Prediction (MinPred, q 0.1) = 1.16 + (0.33 x *FHL2*_C4) + (0.47 x *TRIM59*_C7) + (1.93 x *KLF14*_C3).

Maximum Prediction (MaxPred, q 0.9) = −2.55 + (0.79 x *FHL2*_C4) - (0.06 x *TRIM59*_C7) + (2.28 x *KLF14*_C3).

The final cartilage age prediction model M3 is freely available from the open-access Snipper forensic classification website described in Material and Methods.

3.3. CpG selection for the inference of the tissue of origin

In addition to the 181 cartilage samples, the 44 CpGs located in *KLF14*, *TRIM59*, *MIR29B2CHG, FHL2*, *ELOVL2*, *EDARADD, PDE4C* and *ASPA* were also analyzed in 125 blood samples, 122 buccal swabs and 156 bone samples, using DNA methylation data gathered in Woźniak et al. The corresponding DNA methylation data can be found in Supplementary Table S3. The corresponding dispersion diagrams are shown in Supplementary Fig. S2 and the mean DNA methylation values per tissue for all 44 CpG sites in Supplementary Table S4. The DNA methylation levels for two of the genes previously discarded for age estimation – *MIR29B2CHG* and *EDARADD* – showed a marked difference between cartilage samples and the remaining somatic tissues. The three CpG sites analyzed for *MIR29B2CHG* (C1, C2 and C3) showed continuous patterns of methylation of about ~10–60% (mean: 33.81%) in cartilage samples, while higher methylation levels were found for blood (mean: 75.01%), buccal cells (mean: 78.53%) and bone (mean: 85.17%). The opposite pattern was detected in *EDARADD* (C1 and C2). Continuous hypermethylation was observed in cartilage samples (mean: 83.47%), whereas the additional somatic tissues had lower levels of methylation (mean: 38.75%). The *ASPA* gene previously discarded for age estimation, was informative for blood samples with the highest differences in DNA methylation values (mean: 72.16%) compared to other somatic tissues (mean: 32.51%). In genes *KLF14*, *TRIM59*, *FHL2*, *ELOVL2* and *PDE4C*, patterns of tissue differentiation were evident in most of the CpGs in these genes. In the case of *KLF14*, C1 gave the highest differences in DNA methylation levels between bone (mean: 12.9%) and other tissues (mean: 6.5%). In *TRIM59*, although some overlapping values were detected between blood and buccal cells for young individuals, methylation differences were observed among the four tissues – blood, buccal cells, bone, and cartilage – for C1 (mean: 25.73%, 34.82%, 14% and 7.3%, respectively), C2 (mean: 20.49%, 28.25%, 9.93% and 5.62%, respectively), C3 (mean: 29.92%, 46.35%, 17.32% and 12.74%, respectively), C4 (mean: 47.22%, 61.37%, 29.07% and 18.85%, respectively) and C5 (mean: 45.99%, 62.13%, 26.58% and 19.27%, respectively); while C3, C6, C7 and C8 had overlapping values between bone and cartilage. In *FHL2*, the highest differences in DNA methylation levels were detected between blood samples and other tissues (difference in DNA methylation levels for blood versus the remaining tissues: 32.92%, 34.09%, 33.04%, 34.11%, 30.19%, 29.54%, 16.32%, 13.65%, 28.36% and 8.97%, from C1 to C10, respectively). The differentiation of buccal cells was also achieved with *FHL2*, but partially, since a portion of samples had marked levels of hypomethylation, but the remaining proportion overlapped with bone and cartilage. *ELOVL2* had methylation differences among the four tissues for all the C1 to C9 analyzed CpGs (mean: 49.53%, 63.33%, 28.15% and 16.85% for blood, buccal cells, bone, and cartilage, respectively). In *PDE4C*, simultaneous differentiation of the four tissues was mainly shown by C3 (mean: 33.36%, 25.1%, 11.91% and 7.01%, for blood, buccal cells, bone, and cartilage, respectively).

To select the most informative CpGs, each marker was assessed using multinomial logistic regression. Supplementary Table S5 shows the corresponding mean percentage of correct classifications for all the 44 CpGs analyzed in the eight genes. The following CpGs gave the highest rate of correct classifications per gene and were selected for further analyses: *EDARADD*_C1 (76.37%), *TRIM59*_C1 (76.54%), *ELOVL2*_C6 (72.09%), *MIR29B2CHG*_C3 (71.4%), *PDE4C*_C3 (70.03%), *ASPA*_C1 (63.53%), *FHL2*_C10 (61.3%) and *KLF14*_C1 (51.2%). These eight CpG sites were then selected to build a tissue prediction model.

3.4. A multinomial logistic prediction model for somatic tissue differentiation

Based on the DNA methylation differences amongst different tissues outlined above, a tissue prediction model was developed using logistic regression. In order to build the model, a training set of 392 samples was assessed (n = 87 blood samples, n = 86 buccal swabs, n = 110 bone and n = 109 cartilage samples). Using this training set, a total of eight statistical models based on multinomial logistic regression were tested with one-step increases in the number of CpG sites included (M1, M2, M3, M4, M5, M6 and M7 and M8). Table 2 shows the corresponding cross-validation performance metrics for the training set for the eight evaluated models. The CpG sites were serially included in the models following a decreasing order of correct classification rate, as described above. Using this approach, the CpG site providing the highest level of correct classifications was evaluated in the first model M1 (*EDARADD*_C1) correctly classifying 77.3% of the samples and showing a sensitivity of 0.76 and a specificity of 0.924. Each time an additional CpG site was incorporated into the model, including *TRIM59*_C1 in M2, *ELOVL2*_C6 in M3, *MIR29B2CHG*_C3 in M4, *PDE4C*_C3 in M5, *ASPA*_C1 in M6, *FHL2*_C10 in M7 and *KLF14*_C1 in M8; the rate of correct classifications increased to reach a maximum of 98.72% for M8 (all the eight CpGs sites included), as well as 0.988 for sensitivity and 0.996 for specificity, so M8 was selected as the final tissue prediction model. Listed per tissue, the following results were obtained for blood (98.85% correct classification, 0.989 sensitivity, 0.993 specificity), for buccal swabs (%CC: 100%, sensitivity: 1 specificity: 0.997), for bone (%CC: 96.36%, sensitivity: 0.964 specificity: 1) and for cartilage samples (%CC: 100%, sensitivity: 1 specificity: 0.993). Principal Component Analysis (PCA) results based on the eight CpGs (*EDARADD*_C1, *TRIM59*_C1, *ELOVL2*_C6, *MIR29B2CHG*_C3, *PDE4C*_C3, *ASPA*_C1, *FHL2*_C10 and *KLF14*_C1) are plotted in Fig. 2A. Blood samples, buccal swabs, bone, and cartilage samples are represented as red, orange, violet and green datapoints, respectively. The first Principal Component (PC1) explains 49.7% of tissue separation, and the second, PC2, 27.9%. To validate the tissue prediction model, a test set of 192 samples (n = 38 blood samples, n = 36 buccal swabs, n = 46 bone and n = 72 cartilage samples) was assessed and gave 97.4% correct classifications, a sensitivity of 0.968 and specificity of 0.991. Listed per tissue these gave the following values for blood (%CC: 97.3%, sensitivity: 0.973 specificity: 0.987), for buccal swabs (%CC: 89.74%, sensitivity: 0.897 specificity: 0.993), for bone (%CC: 100%, sensitivity: 1 specificity: 0.993) and for cartilage samples (%CC: 100%, sensitivity: 1 specificity: 0.992). The corresponding PCA is shown in Fig. 2B. The main difference in comparison to the training set was the decrease in the classification rate for buccal swabs (from 100% to 89.74%). This is due to four misclassifications (two samples predicted as blood, one sample as bone and one as cartilage). The remaining tissues gave similar classification rates between the training and testing sets. The final tissue prediction model is freely available from the open-access Snipper forensic classification website described in Material and Methods.

Table 2
Predictive performance metrics for the training (cross-validation) and testing set for the somatic tissue prediction model developed using multinomial logistic regression (blood vs buccal cells vs bone vs cartilage samples). $\%CC_{mean}$ (mean of the percent of correct classifications). Bold indicates the selected model.

	Model	CpG nº	CpG_ID	$\%CC_{mean}$	$Sensitivity_{mean}$	$Specificity_{mean}$
Training tissue (n = 392)	M1	1	*EDARADD*_C1	77.3%	0.76	0.924
	M2	2	*EDARADD*_C1 *TRIM59*_C1	86.97%	0.862	0.957
	M3	3	*EDARADD*_C1 *TRIM59*_C1 *ELOVL2*_C6	89.28%	0.884	0.965
	M4	4	*EDARADD*_C1 *TRIM59*_C1 *ELOVL2*_C6 *MIR29B2CHG*_C3	91.84%	0.913	0.973
	M5	5	*EDARADD*_C1 *TRIM59*_C1 *ELOVL2*_C6 *MIR29B2CHG*_C3 *PDE4C*_C3	96.18%	0.958	0.987
	M6	6	*EDARADD*_C1 *TRIM59*_C1 *ELOVL2*_C6 *MIR29B2CHG*_C3 *PDE4C*_C3 *ASPA*_C1	96.68%	0.965	0.989
	M7	7	*EDARADD*_C1 *TRIM59*_C1 *ELOVL2*_C6 *MIR29B2CHG*_C3 *PDE4C*_C3 *ASPA*_C1 *FHL2*_C10	98.21%	0.98	0.994
	M8	**8**	***EDARADD*_C1** ***TRIM59*_C1** ***ELOVL2*_C6** ***MIR29B2CHG*_C3** ***PDE4C*_C3** ***ASPA*_C1** ***FHL2*_C10** ***KLF14*_C1**	**98.72%**	**0.988**	**0.996**
Test tissue (n = 192)	**M8**	**8**	***FHL2*_C4** ***TRIM59*_C7** ***KLF14*_C3**	**97.4%**	**0.968**	**0.991**

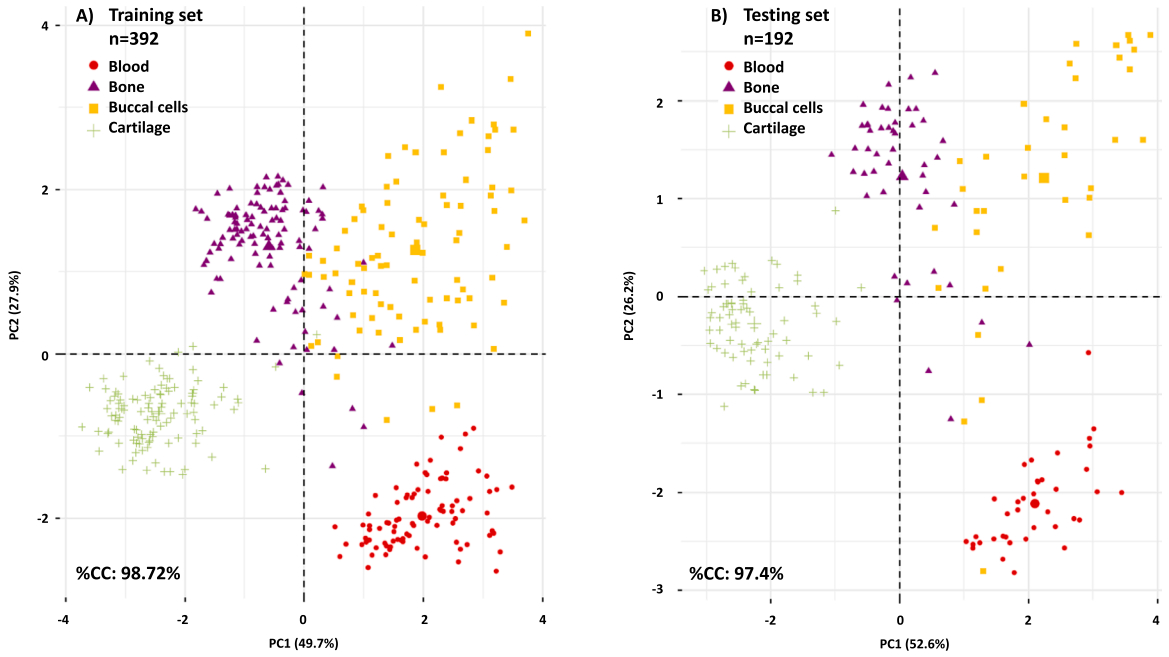

Fig. 2. Principal Component Analysis (PCA) based on eight CpGs (*EDARADD*_C1, *TRIM59*_C1, *ELOVL2*_C6, *MIR29B2CHG*_C3, *PDE4C*_C3, *ASPA*_C1, *FHL2*_C10 and *KLF14*_C1) for A) the training (n = 392: 109 cartilage samples, 110 bone samples, 87 blood samples and 86 buccal swabs) and B) the testing set (n = 192: 72 cartilage samples, 46 bone samples, 38 blood samples and 36 buccal swabs). Blood samples, buccal swabs, bone, and cartilage are depicted as red, orange, violet and green datapoints, respectively.

4. Discussion

Age estimation using epigenetic markers has been widely explored during the last ten years [40]. The observation of high correlation of DNA methylation levels with chronological age has been translated into a large list of age prediction models. Since DNA methylation is tissue-dependent, models are usually developed based on specific tissues. Indeed, to date, age estimation has been mainly focused on the most commonly analyzed forensic tissues such as blood [41,42], buccal cells [43], saliva [44], semen [45,46] or nails [47]. Nevertheless, skeletal remains are also important sources of biological material for both forensic and anthropological analyses. To address such DNA analyses, several studies have introduced age prediction models for teeth and bone [48–50]. Although at the moment multiple age prediction models can be found in the literature, few provide coverage for various tissues at the same time. Ten years ago, Horvath reported the first pan-tissue epigenetic clock applicable to 51 tissues and cell types [28], five of them forensically relevant: blood, buccal cells, saliva, epidermis and knee cartilage. However, the Horvath model needs DNA methylation data for 353 CpG sites that is not useful when working with DNA samples of poor quality and quantity common to forensic analysis. In order to solve this constrain, in 2019, Jung et al. introduced the first forensic tissue-combined model for age inference covering three somatic tissues – blood, saliva and buccal swabs – using capillary electrophoresis [31]. Two years later, the VISAGE Enhanced Tool was developed based on massively parallel sequencing, designed to estimate age from blood and buccal cells, as well as bone samples [32].

Regarding additional forensic specimens affected by decomposition, an initial attempt to infer age was recently undertaken by Becker et al. [51]. In this study, age estimation for elastic cartilage from the epiglottis was explored using a protein clock based on racemization of aspartic acid and accumulation of pentosidine, which provided an MAE of ± 4 years. Moreover, costal cartilage samples were also explored using the age prediction model developed for bone generated with the VISAGE Enhanced Tool [32]. Nevertheless, high prediction errors were obtained (MAE: ± 25.8 years for cartilage samples compared to ± 3.4 years for bone) [32], thus justifying our development of an age prediction model specifically for cartilage.

To the best of our knowledge, this is the first study reporting forensic age estimation for cartilage based on DNA methylation. To establish an efficient predictive model, the VISAGE Enhanced Tool comprising a total of 44 CpG sites located in eight genes (*KLF14*, *TRIM59*, *MIR29B2CHG, FHL2*, *ELOVL2*, *EDARADD, PDE4C* and *ASPA*) has been explored in 181 costal cartilage samples representing a full adult age range [32]. From these candidates, three CpG sites from three genes were selected to build the cartilage-specific age prediction model using multivariate quantile regression (*FHL2*_C4, *TRIM59*_C7 and *KLF14*_C3). Cross-validation of the model provided an MAE of ± 4.41 years and RMSE of 5.52. When assessing this tool in an independent test set, comparable results were obtained (MAE: ± 4.26 years, RMSE: 5.39), which were also similar to the values obtained from the protein clock-based system reported by Becker et al. (MAE: ± 4.0 years) [51]. However, prediction errors for the cartilage model were slightly higher if comparing with other epigenetic clocks generated from the VISAGE Enhanced Tool for blood (MAE: ± 3.2 years), buccal cells (MAE: ± 3.7 years) and bone (MAE: ± 3.4 years) [32]. When plotting the predicted age against chronological age (Fig. 1), a slight overestimation of age in young samples as well as an underestimation in older ones was observed, especially in the test set, which indicates the utility of age-specific prediction intervals compared to the predicted age. Although both training and test sets have similar age range distributions, this effect could be explained by a reduced sample size (n = 109 and n = 72, for training and test sets, respectively). However, due to the nature of the specimens, broadly-based sample collection for a complete age range is difficult to achieve.

As a supplementary analysis to age estimation, identification of the biological source of a stain using DNA methylation analysis becomes a useful application in forensic genetics. The initial development of the VISAGE Enhanced Tool for age prediction from somatic tissues allowed the inference of the epigenetic age of somatic tissues such as blood, buccal cells and bone [32], which is now extended to cartilage samples. To broaden the applications of this MPS tool, a tissue prediction model was additionally developed. DNA methylation has previously shown its potential for tissue identification based on the fact that this epigenetic signature affects gene expression and therefore, genomic loci are

differentially methylated between tissues. However, selection of previous markers was exclusively made to accomplish tissue differentiation [52–54]. Moreover, assessment of such assays was based on the detection of the marker presenting the methylated signal, leading to a direct assignment to the corresponding tissue of origin. In the present model, a quantitative rather than a qualitative evaluation was applied. Therefore, the novelty of this assay consists not only in simultaneous use of the VISAGE Enhanced Tool for inference of age and tissue source, but on developing a different approach for the latter. From the 44 CpG sites analyzed, eight markers were selected to build the tissue prediction model using multinomial logistic regression (*EDARADD*_C1, *TRIM59*_C1, *ELOVL2*_C6, *MIR29B2CHG*_C3, *PDE4C*_C3, *ASPA*_C1, *FHL2*_C10 and *KLF14*_C1), classifying blood, buccal cells, bone, and cartilage. Although not all the eight markers contributed to a full separation of the four tissues, cross-validation of the 8-CpG combined model provided 98.72% correct classifications, with high sensitivity (0.988) and specificity (0.996) values. The assessment of an independent testing set led to similar results of 97.4% of correct classifications, 0.968 for sensitivity and 0.991 for specificity.

To date, methods for body fluid identification have largely relied on chemical or immunological tests [55]. However, lack of specificity and requirements for large amounts of sample related to these methods can be solved using epigenetic markers. In this way, through a single reaction, differentiation of four potential tissue sources can be achieved. Since it is relevant to detect the presence of body fluids or tissues in biological specimens, differentiation between blood and buccal cells can add a determinant value to the forensic investigations. However, differentiation between cartilage and bone is much less critical for forensic purposes, since sample collection determines per se the origin of the sample. Differences between cartilage and bone in *EDARADD* have been previously found in other animal species, such as Baboons [56]. Although from a forensic point of view, the differentiation of cartilage and bone is largely unnecessary; we note that epigenetic differences between both tissues could be useful in clinical applications when studying the development of degenerative diseases such as osteoarthritis [57].

Declaration of Competing Interest

The authors have declared no conflict of interest.

Acknowledgements

This study received support from the European Union's Horizon 2020 Research and Innovation Program under grant agreement No. 740580 within the framework of the Visible Attributes through Genomics (VISAGE) Project and Consortium and form an institutional grant for young scientists from the Medical University of Silesia in Katowice, Poland (grant no. PCN-2-053/K/2/O).

Appendix A. Supporting information

Supplementary data associated with this article can be found in the online version at doi:10.1016/j.fsigen.2023.102936.

References

[1] M.D. Vigeland, T. Egeland, Joint DNA-based disaster victim identification, Sci. Rep. 11 (2021), 13661.
[2] M. Prinz, A. Carracedo, W.R. Mayr, N. Morling, T.J. Parsons, A. Sajantila, et al., DNA commission of the international society for forensic genetics (ISFG): recommendations regarding the role of forensic genetics for disaster victim identification (DVI), Forensic Sci. Int. Genet. 1 (1) (2007) 3–12.
[3] G. Calacal, F. Delfin, M. Tan, L. Roewer, D. Magtanong, M. Lara, et al., Identification of exhumed remains of fire tragedy victims using conventional methods and autosomal/Y-chromosomal short tandem repeat DNA profiling, Am. J. Forensic Med. Pathol. 26 (3) (2005) 285–291.
[4] A. Ossowski, M. Kuś, P. Brzeziński, J. Prüffer, J. Piątek, G. Zielińska, et al., Example of human individual identification from World War II gravesite, Forensic Sci. Int. 233 (1–3) (2013) 179–192.
[5] M. Baeta, C. Núñez, S. Cardoso, P.-M. L, L. Herrasti, F. Etxeberria, et al., Digging up the recent Spanish memory: genetic identification of human remains from mass graves of the Spanish Civil War and posterior dictatorship, Forensic Sci. Int. Genet. 19 (2015) 272–279.
[6] M. Alvarez-Cubero, M. Saiz, L. Martinez-Gonzalez, J. Alvarez, A. Eisenberg, B. Budowle, et al., Genetic identification of missing persons: DNA analysis of human remains and compromised samples, Pathobiology 79 (5) (2012) 228–238.
[7] A. Nadeem, M. Ashraf, N. Qadeer, K. Rizwan, A. Mehmood, A. AlZahrani, et al., Tracking missing person in large crowd gathering using intelligent video surveillance, Sensors 22 (14) (2022) 5270.
[8] National Crime Information Center - FBI, Criminal Justice Information Service (CJIS), Missing Pers. Unidentified Pers. Stat. (2021). ⟨https://www.fbi.gov/file-repository/2021-ncic-missing-person-and-unidentified-person-statistics.pdf/view⟩.
[9] https://www.interpol.int/News-and-Events/News/2021/INTERPOL-unveils-new-global-database-to-identify-missing-persons-through-family-DNA.
[10] M. Tomsia, K. Droździok, G.T. Javan, R. Skowronek, M. Szczepański, E. Chełmecka, Costal cartilage ensures low degradation of DNA needed for genetic identification of human remains retrieved at different decomposition stages and different postmortem intervals, Post. Hig. i Med Doświadczalnej / Adv. Hyg. Exp. Med 75 (2021) 852–858.
[11] M. Tomsia, Kornelia Droździok, P. Banaszek, M. Szczepański, A. Pałasz, E. Chełmecka, The intervertebral discs' fibrocartilage as a DNA source for genetic identification in severely charred cadavers, Forensic Sci. Med Pathol. 18 (2022) 442–449.
[12] J. Becker, N. Mahlke, S. Ritz-Timme, P. Boehme, The human intervertebral disc as a source of DNA for molecular identification, Forensic Sci. Med. Pathol. 17 (4) (2021) 660–664. Available from: papers2://publication/uuid/AA4D3970-F698-408D-9644-5827F2A2141B.
[13] M.L. Goff, Early postmortem changes and stages of decomposition, Exp. Appl. Acarol. 49 (1–2) (2009) 21–36.
[14] T. Siriboonpiputtana, T. Rinthachai, J. Shotivaranon, V. Peonim, B. Rerkamnuaychoke, Forensic genetic analysis of bone remain samples, Forensic Sci. Int. 284 (2018) 167–175.
[15] J. Jakubowska, A. Maciejewska, R. Pawłowski, Comparison of three methods of DNA extraction from human bones with different degrees of degradation, Int. J. Leg. Med. 126 (1) (2012) 173–178.
[16] Y. Seo, D. Uchiyama, K. Kuroki, T. Kishida, STR and mitochondrial DNA SNP typing of a bone marrow transplant recipient after death in a fire, Leg. Med. 14 (6) (2012) 331–335.
[17] Sanz-Piña, E. Santurtún, A. Zarrabeitia, M. Sanz-Piña, et al., Forensic Sci. Int 2019 (2019) 302, 109862.
[18] M. Tomsia, J. Ciesla, Joanna Pilch-Kowalczyk, Przemysław Banaszek, E. Chełmecka, Cartilage tissue in forensic science—state of the art and future research directions, Processes 10 (2022) 2456.
[19] M. Tomsia, M. Głaz, J. Nowicka, M. Szczepanski, Sodium nitrite detection in costal cartilage and vitreous humor – Case report of fatal poisoning with sodium nitrite, J. Forensic Leg. Med. 81 (2021), 102186.
[20] M. Tomsia, J. Nowicka, R. Skowronek, M. Woś, J. Wójcik, K. Droździok, et al., A comparative study of ethanol concentration in costal cartilage in relation to blood and urine, Processes 8 (2020) 1637.
[21] M. Tomsia, J. Nowicka, R. Skowronek, G.T. Javan, E. Chełmecka, Concentrations of volatile substances in costal cartilage in relation to blood and urine – preliminary studies, Arch. Med. Sadowej Kryminol. 71 (1–2) (2021) 38–46.
[22] J. Hardy, S. Chrosciany, J. Bernard, C. Mabit, P. Marcheix, The human costal cartilage: Anatomical and radiological study of macro-vascularization and micro-vascularization and its clinical relevance regarding vascularized chondrocostal free flap surgery, Ann. Anat. 232 (2020), 151581.
[23] E. Safronova, N. Borisova, S. Mezentseva, K. Krasnopol'skaya, Characteristics of the macromolecular components of the extracellular matrix in human hyaline cartilage at different stages of ontogenesis, Biomed. Sci. 2 (2) (1991) 162–168.
[24] H. Pfeiffer, H. Mörnstad, A. Teivens, Estimation of chronologic age using the aspartic acid racemization method. I. On human rib cartilage, Int. J. Leg. Med. 108 (1) (1995) 19–23.
[25] T. Ikeda, Estimating age at death based on costal cartilage calcification, Tohoku J. Exp. Med. 243 (4) (2017) 237–246.
[26] S. Zhang, J. Zhen, H. Li, S. Sun, H. Wu, P. Shen, et al., Characteristics of Chinese costal cartilage and costa calcification using dual-energy computed tomography imaging, Sci. Rep. 7 (2017), 2923.
[27] J. Fernández-Tajes, A. Soto-Hermida, M. Vázquez-Mosquera, E. Cortés-Pereira, A. Mosquera, M. Fernández-Moreno, N. Oreiro, C. Fernández-López, et al., Genome-wide DNA methylation analysis of articular chondrocytes reveals a cluster of osteoarthritic patients, Ann. Rheum. Dis. 73 (4) (2014) 668–677.
[28] S. Horvath, DNA methylation age of human tissues and cell types, Genome Biol. 14 (10) (2013) R115.
[29] K. Alkass, B.A. Buchholz, S. Ohtani, T. Yamamoto, H. Druid, K.L. Spalding, Age estimation in forensic sciences: application of combined aspartic acid racemization and radiocarbon analysis, Mol. Cell Proteom. 9 (5) (2010) 1022–1030.
[30] A. Pisarek, E. Pośpiech, A. Heidegger, C. Xavier, A. Papież, D. Piniewska-Róg, et al., Epigenetic age prediction in semen - marker selection and model development, Aging 13 (15) (2021) 19145–19164.
[31] S.E. Jung, S.M. Lim, S.R. Hong, E.H. Lee, K.J. Shin, H.Y. Lee, DNA methylation of the ELOVL2, FHL2, KLF14, C1orf132/MIR29B2C, and TRIM59 genes for age

prediction from blood, saliva, and buccal swab samples, Forensic Sci. Int. Genet. 38 (2019) 1–8.
[32] A. Woźniak, A. Heidegger, D. Piniewska-róg, E. Pośpiech, A. Pisarek, E. Kartasińska et al., Development of the VISAGE Enhanced Tool and statistical models for epigenetic age estimation in blood, buccal cells and bones 13 5 2021.
[33] B. Koop, F. Mayer, T. Gündüz, J. Blum, J. Becker, J. Schaffrath, et al., Postmortem age estimation via DNA methylation analysis in buccal swabs from corpses in different stages of decomposition-a "proof of principle" study, Int J. Leg. Med 135 (1) (2021) 167–173.
[34] D.R. Masser, A.S. Berg, W.M. Freeman, Focused, high accuracy 5-methylcytosine quantitation with base resolution by benchtop next-generation sequencing, Epigenetics Chromatin 6 (1) (2013), 33.
[35] R. Koenker, S. Portnoy, P.T. Ng, A. Zeileis, P. Grosjean, C. Moler et al., Quantile Regres., Package "quantreg. " 2019.
[36] H. Wickham, W. Chang, Creat. Elegant Data Vis. Using Gramm. Graph., Package "ggplot2. " 2019.
[37] B. Ripley, W. Venables, Feed-Forw. Neural Netw. Multinomial Log. -Linear Models, Package "nnet. " 2022.
[38] A. Kassambara, F. Mundt, Extr. Vis. Results Multivar. Data Anal., Package "factoextra. " 2022.
[39] A. Alfons Cross-Valid. tools Regres. Models, Package "cvTools. " 2015.
[40] R. Noroozi, S. Ghafouri-Fard, A. Pisarek, J. Rudnicka, M. Spólnicka, W. Branicki, et al., DNA methylation-based age clocks: from age prediction to age reversion, Ageing Res Rev. 68 (2021), 101314.
[41] R. Zbieć-Piekarska, M. Spólnicka, T. Kupiec, A. Parys-Proszek, Z. Makowska, A. Pałeczka, et al., Development of a forensically useful age prediction method based on DNA methylation analysis, Forensic Sci. Int. Genet. 17 (2015) 173–179.
[42] A. Freire-Aradas, L. Girón-Santamaría, A. Mosquera-Miguel, A. Ambroa-Conde, C. Phillips, M. Casares de Cal, et al., A common epigenetic clock from childhood to old age, Forensic Sci. Int. Genet. 60 (2022), 102743.
[43] A. Ambroa-Conde, L. Girón-Santamaría, A. Mosquera-Miguel, C. Phillips, M. A. Casares de Cal, A. Gómez-Tato, et al., Epigenetic age estimation in saliva and in buccal cells, Forensic Sci. Int. Genet. 61 (2022), 102770.
[44] S.R. Hong, S.E. Jung, E.H. Lee, K.J. Shin, W.I. Yang, H.Y. Lee, DNA methylation-based age prediction from saliva: High age predictability by combination of 7 CpG markers, Forensic Sci. Int. Genet. 29 (2017) 118–125.
[45] H.Y. Lee, S.E. Jung, Y.N. Oh, A. Choi, W.I. Yang, K.J. Shin, Epigenetic age signatures in the forensically relevant body fluid of semen: a preliminary study, Forensic Sci. Int. Genet. 19 (2015) 28–34.
[46] A. Heidegger, A. Pisarek, M. de la Puente, H. Niederstätter, E. Pośpiech, A. Woźniak, et al., Development and inter-laboratory validation of the VISAGE enhanced tool for age estimation from semen using quantitative DNA methylation analysis, Forensic Sci. Int. Genet. 56 (2022), 102596.
[47] K. Fokias, L. Dierckx, W. Van de Voorde, B. Bekaert, Age determination through DNA methylation patterns in fingernails and toenails, Forensic Sci. Int. Genet. 16 (64) (2023), 102846.
[48] B. Bekaert, A. Kamalandua, S.C. Zapico, W. Van De Voorde, R. Decorte, Improved age determination of blood and teeth samples using a selected set of DNA methylation markers, Epigenetics 10 (10) (2015) 922–930.
[49] H. Correia Dias, L. Manco, F. Corte Real, E. Cunha, A blood–bone–tooth model for age prediction in forensic contexts, Biology 10 (12) (2021) 1312.
[50] H.Y. Lee, S.R. Hong, J.E. Lee, I.K. Hwang, N.Y. Kim, J.M. Lee, et al., Epigenetic age signatures in bones, Forensic Sci. Int. Genet. 46 (2020).
[51] J. Becker, N.S. Mahlke, A. Reckert, S.B. Eickhoff, S. Ritz-Timme, Age estimation based on different molecular clocks in several tissues and a multivariate approach: an explorative study, Int. J. Leg. Med. 134 (2) (2020) 721–733.
[52] H. Lee, J. An, S. Jung, Y. Oh, E. Lee, A. Choi, et al., Genome-wide methylation profiling and a multiplex construction for the identification of body fluids using epigenetic markers, Forensic Sci. Int. Genet. 17 (2015) 17–24.
[53] D. Silva, J. Antunes, K. Balamurugan, G. Duncan, C. Alho, B. McCord, Developmental validation studies of epigenetic DNA methylation markers for the detection of blood, semen and saliva samples, Forensic Sci. Int. Genet. 23 (2016) 55–63.
[54] H. Holtkötter, V. Beyer, K. Schwender, A. Glaub, K. Johann, M. Schürenkamp, et al., Independent validation of body fluid-specific CpG markers and construction of a robust multiplex assay, Forensic Sci. Int. Genet. 29 (2017) 261–268.
[55] T. Sijen, S. Harbison, On the identification of body fluids and tissues: a crucial link in the investigation and solution of crime, Genes 12 (11) (2021) 1728.
[56] G. Housman, E.E. Quillen, A.C. Stone, An evolutionary perspective of DNA methylation patterns in skeletal tissues using a baboon model of osteoarthritis, J. Orthop. Res. 39 (10) (2021) 2260–2269.
[57] Jb van Meurs, C. Boer, L. Lopez-Delgado, J. Riancho, Role of epigenomics in bone and cartilage disease, J. Bone Min. Res. 34 (2) (2019) 215–230.